



# Role of $\beta$ -cyclodextrin nanosponges in polypropylene photooxidation

Jenny Alongi<sup>a,\*</sup>, Merima Poskovic<sup>a</sup>, Alberto Frache<sup>a</sup>, Francesco Trotta<sup>b</sup>

<sup>a</sup> Dipartimento di Scienza dei Materiali e Ingegneria Chimica, Politecnico di Torino, sede di Alessandria, Viale Teresa Michel 5, 15121 Alessandria, Italy

<sup>b</sup> Facoltà di Scienze Matematiche, Fisiche e Naturali, Università di Torino, Via Verdi 8, 10124 Torino, Italy

## ARTICLE INFO

### Article history:

Received 28 February 2011

Received in revised form 27 March 2011

Accepted 11 April 2011

Available online 16 April 2011

### Keywords:

Cyclodextrins

Nanosponges

Photooxidation

Polypropylene

## ABSTRACT

The interactions between  $\beta$ -cyclodextrin nanosponges and two different UV stabilizers (namely, 2-hydroxy-4(octyloxy)-benzophenone and triphenyl phosphite) in the photooxidation of polypropylene exposed to UV light have been investigated. A significant decrease of the oxidation induction time (OIT) has been observed in presence of  $\beta$ -cyclodextrin nanosponges. On the contrary, the combination of the above nanosponges with 2-hydroxy-4(octyloxy)-benzophenone turned out to be very efficient and advantageous since a remarkable increase of OIT has been registered, namely a threefold increase of polypropylene OIT. This result has indicated a possible synergistic effect between the two species due to the occurring of some chemical or physical interactions, verified by comparing the experimental results and data calculated on the basis of simple additivity rule. Some hypotheses on the interaction mechanism between the two species have been given. Conversely, no effect has been found for the triphenyl phosphite–nanosponge pair.

© 2011 Elsevier Ltd. All rights reserved.

## 1. Introduction

Nowadays, the constantly growing demand to develop novel polymers or composites with attractive properties has affected remarkably both the academic and the industrial research activities based on materials engineering. In this scenario, polymer nanocomposites have recently received considerable attention since the successful attempts to develop a montmorillonite-reinforced polyamide 6 by Toyota group (Kojima et al., 1993). Indeed, this relatively new class of materials shows a wide variety of desirable properties compared to both neat polymers and conventional composites because of the nanometric size dispersed particles. Among the numerous properties that can be modified by a very low inorganic content ( $\leq 5$  wt.%), the observed improvements include increased moduli and tensile strength, heat resistance, and decreased gas permeability and flammability (Okada & Usuki, 2006; Pinnavaia & Beall, 2001; Ray & Okamoto, 2003). In the last decade, specific attention of the researchers has been focused on the possibility to exploit nanocomposite materials with the aim of increasing the UV stability of polymers under natural or accelerated conditions. Such polymers, as polypropylene (Bocchini, Morlat-Therias, Gardette, & Camino, 2007; Bocchini, Morlat-Therias, Gardette, & Camino, 2008; Diagne, Gueye, Vidal, & Tidjani, 2005; Diagne, Gueye, Dasilva, Vidal, & Tidjani, 2006; Diagne, Gueye, Dasilva, & Tidjani, 2007; Ding & Qu, 2006; Lonkar, Therias, Caperaa, Leroux,

& Gardette, 2010; Morlat, Maihot, Gonzalez, & Gardette, 2004; Morlat-Therias, Mailhot, Gonzalez, & Gardette, 2005a; Qin et al., 2005), polyethylene (Qin, Zhao, Zhang, Chen, & Yang, 2003; Qin et al., 2004; Morlat-Therias et al., 2008; Magagula, Nhalpo, & Focke, 2009; Kumanayaka, Parthasarathy, & Jollands, 2010) and their blends (Botta, Dintcheva, & La Mantia, 2009) or copolymers (Morlat-Therias et al., 2005b), polystyrene (Bottino, Di Pasquale, Fabbri, Orestano, & Pollicino, 2009; Leroux, Meddar, Mailhot, Morlat-Therias, & Gardette, 2005), polyurethanes (Mailhot et al., 2008), epoxy resins (Chen, Wang, Liao, Mai, & Zhang, 2007) and polylactic acid (Bocchini et al., 2010), have been blended in bulk with some natural or organo-modified montmorillonites, hydro-talcites, bohemites, silica and titania. The effect of these novel additives has been thoroughly investigated; in particular, their role on polymer photooxidation has been evaluated from the chemical and physical interaction point of view.

As far as polyolefins are considered, the most relevant results published in the literature are all in agreement and have shown that nanoparticles (regardless of the type) are responsible of the accelerated photodegradation of polypropylene and polyethylene. For example, referring to montmorillonite-based nanocomposites, Morlat-Therias et al. (2005a) in very detailed papers (Morlat et al., 2004) have recently tried to explain the mechanism by which nanoparticles can affect polyolefin degradation by evaluating relevant aspects of the phenomenon, such as the influence of compatibilizing agent in nanoclays (Morlat et al., 2004) or the interactions between nanoclays and antioxidants (Morlat-Therias et al., 2005a). Their results reveal that the presence of clay and its compatibilizer (alkylammonium cations) dramatically modifies

\* Corresponding author. Tel.: +39 0131 229399; fax: +39 0131 229337.

E-mail address: [jenny.alongi@polito.it](mailto:jenny.alongi@polito.it) (J. Alongi).

polymer oxidation, leading to a shortening of the induction time. Namely, the efficiency of the stabilizer introduced in the polymer matrix turns out to be strongly reduced due to: (i) the degradation of alkylammonium cations in the clay, which can be sensitive sites in terms of radical initiation; and/or (ii) the presence of structural iron as clay impurity, that can have a photocatalytic effect and/or (iii) the adsorption of stabilizer itself onto the clay platelets, which can partially inhibit its activity.

Although it is very difficult to establish a proper hypothesis to explain the loss of polyolefin photostability, the most plausible reason seems to be due to the catalytic effect of iron impurities of nanoclays. Indeed, an analogous study on polyethylene stabilized with different UV antioxidants and metal deactivators has allowed to support this hypothesis (Morlat-Therias et al., 2008). The collected data by Morlat-Therias and coworkers have shown that the most efficient stabilizer in linear low density polyethylene nanocomposites is a metal deactivator, 2-(4,6-bis(2,4-dimethylphenyl)-1,3,5-triazin-2-yl)-5-(octyloxy)phenol (Cyasorb® UV-1164 by Cytec), able to cancel out the photodegradative effect of the iron present in the clay.

The aim of the present work is to study the influence and the role of  $\beta$ -cyclodextrin nanosponges in the photooxidation of polypropylene. The nanosponges employed in the present study have been synthesized by crosslinking  $\beta$ -cyclodextrins (cyclic oligosaccharides formed by 6–8 glucose molecules bonded with a  $\alpha$ -1,4-glycosidic bond, having a characteristic truncated cone structure) in presence of organic carbonates forming a network characterized by both the internal cavities of cyclodextrins and the external holes among nanosponges, as shown in Fig. 1.

These nanoparticles represent a novel class of materials usually obtained by natural derivatives of starch. As compared to the other nanoparticles, they are insoluble both materials in water and organic solvents, porous, non toxic and stable at high temperatures (up to ca. 300 °C). They are able to capture, transport and selectively release a huge variety of substances because of their 3D structure containing cavities of nanometric size and tunable polarity. Furthermore, nanosponges show a remarkable advantage in comparison with the common nanoparticles: indeed, they can be easily regenerated by different treatments, such as washing with eco-compatible solvents, stripping with moderately inert hot gases, mild heating, or changing pH or ionic strength. For all these characteristics, nanosponges have been already employed in different applied fields, such as cosmetic and pharmaceutical sectors (Cavalli, Trotta, & Tumiatto, 2006; Di Nardo et al., 2009; Swaminathan, Vavia, Trotta, & Torne, 2007; Swaminathan et al., 2010a, 2010b; Torne, Ansari, Vavia, Trotta, & Cavalli, 2010), flower cultivation (Boscolo, Trotta, & Ghibaudi, 2010) and flame retardancy of polymers (Alongi, Poskovic, Frache, & Trotta, 2010).

Our study should open a novel field of investigation from the present state of the art, since the nanosponges under evaluation are only based on  $\beta$ -cyclodextrins and, therefore, should not present the same problems of the common nanoparticles linked to iron impurities. Furthermore, having internal and external cavities, they could be able to host and protect UV stabilizers. With this aim, two different kinds of stabilizers (2-hydroxy-4(octyloxy)-benzophenone and triphenyl phosphite) have been mixed with nanosponges, and the synergistic effect of these two species have been assessed in order to understand the possible chemical or phys-

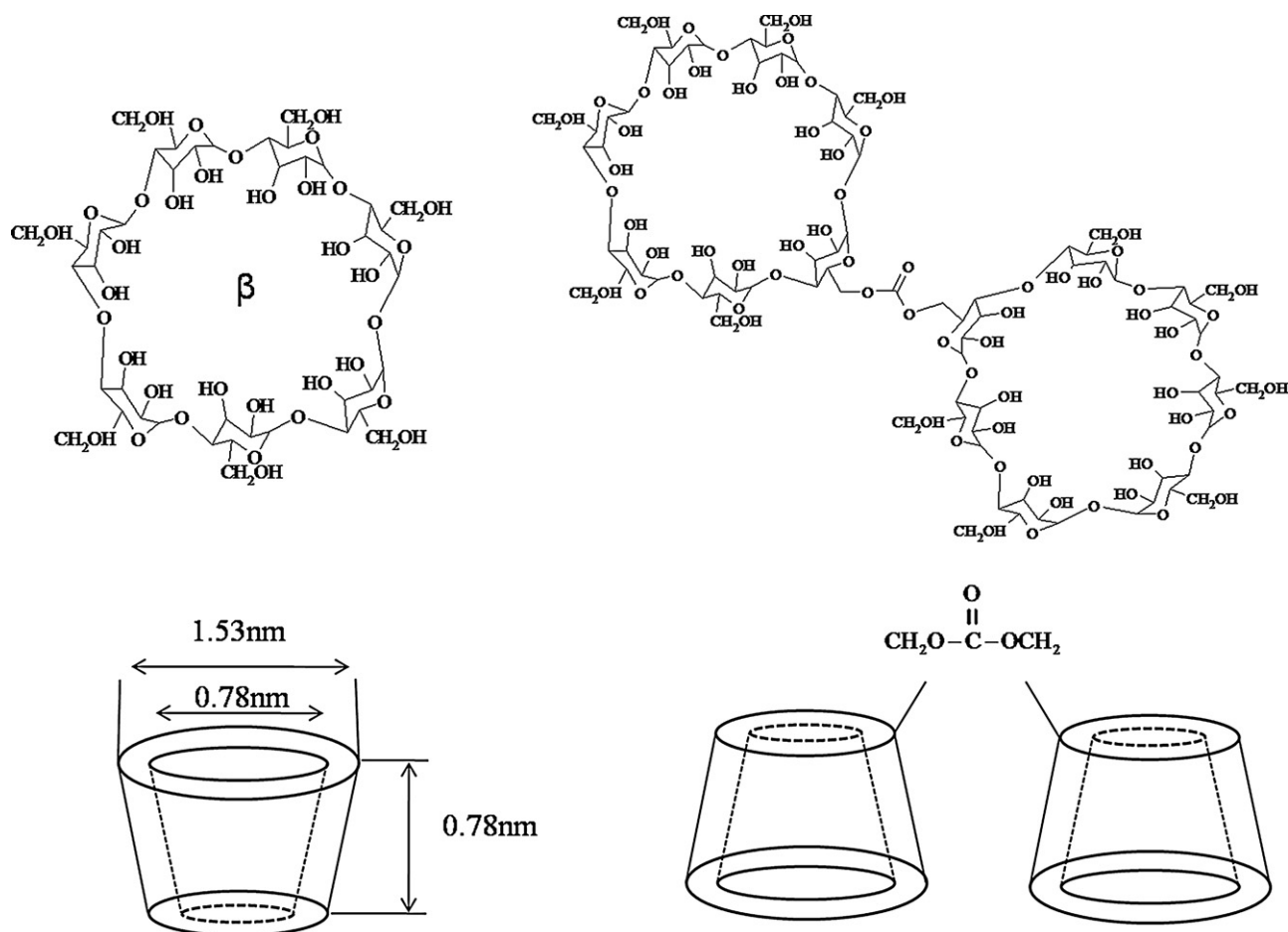
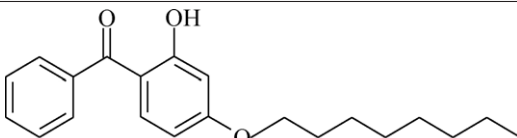
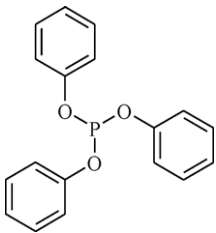


Fig. 1. Chemical structure of  $\beta$ -cyclodextrin unit and  $\beta$ -cyclodextrin nanosponges.

**Table 1**  
UV stabilizers under study.

Code	Name	Chemical structure
HOBP	2-Hydroxy-4(octyloxy)-benzophenone	
TPP	Triphenyl phosphite	

ical interactions occurring between them. Specific attention has been given to the influence of each component on the oxidation of the polymer matrix.

## 2. Experimental part

### 2.1. Materials

Polypropylene (HP500N<sup>®</sup>, highly isotactic, semi-crystalline, nucleated homopolymer, MFI=12 g/10 min following ISO1133 standard) was supplied by Basell S.p.A.  $\beta$ -cyclodextrin nanospheres (NS) were laboratory preparation following the detailed procedure described elsewhere (Alongi et al., 2010). Two different kinds of UV stabilizers, namely 2-hydroxy-4(octyloxy)-benzophenone (HOBP) and triphenyl phosphite (TPP), both reagent grade, were purchased from Sigma Aldrich Inc. and Ciba, respectively and used as received. Their chemical structure is given in Table 1.

### 2.2. Preparation of NS/stabilizer pairs

NS/stabilizer (HOBP or TPP) pairs were prepared by simple mechanical grinding with a weight ratio of 1:1 for NS:HOBP and 2:1 for NS:TPP systems, respectively. The above concentrations were chosen on the basis of preliminary studies carried out in order to optimize this ratio.

### 2.3. Preparation of PP-based composites and films

PP-based composites were prepared by melt blending, mixing PP with NS, or stabilizers, or preformed NS/stabilizer pairs, respectively, using a mini twin screw extruder (MINI TSE DSM Model) at 190 °C, 60 rpm for 4 min. These mixing operations were found to achieve optimum conditions since they guarantee a close interaction between NS and stabilizer. Indeed, for this purpose, a sample containing 0.05 wt.% of NS and 0.05 wt.% of HOBP (PP01NSHOBP\*) was prepared mixing PP and NS and, subsequently, HOBP, without a previous mixing of nanospheres and stabilizer, and compared with the analogous formulation prepared by the first approach (PP01NSHOBP). The prepared formulations are summarized in Table 2.

Films for photooxidation were prepared using a laboratory hydraulic press, i.e. a film-maker machine (Specac Inc.) operating at 190 °C using a pressure of 2.5 ton for 3 min. The film thickness was measured by a micrometer. Sample thickness was maintained

below 25  $\mu$ m, i.e. a thickness that avoids the effect of oxygen permeation on photooxidation rate.

### 2.4. Irradiation

The films were irradiated at  $\lambda > 300$  nm in air at 60 °C in a SEPAP 12/24 unit (ATLAS) by cycle of 4/8 h with total exposition of 100 h. Such apparatus is designed to evaluate the accelerated artificial photodegradation, in conditions similar to natural outdoor weathering (Philippart, Sinturel, & Gardette, 1995) and is equipped with four medium-pressure mercury lamps covered with borosilicate envelope, which filters wavelength below 300 nm.

### 2.5. Characterization

The surface morphology of the prepared samples has been detected using a Scanning Electron Microscope (SEM, LEO 1450VP). Film pieces (0.5 mm  $\times$  0.5 mm) have been fixed to conductive adhesive tapes and gold-metalized.

The photooxidation of the prepared films was followed by infrared and UV-visible spectroscopy. Infrared spectra of films were recorded using a Nicolet 5SX-FTIR spectrometer and the spectra were obtained by 32 scans with a resolution of 4 cm<sup>-1</sup>. The photooxidation process was controlled by infrared spectroscopy monitoring the absorbance band at 1717 cm<sup>-1</sup> which increases as a function of the irradiation time. In order to eliminate any difference due to film thickness, the absorbance was normalized to the IR absorption band at 2723 cm<sup>-1</sup> (characteristic vibration stretching band of PP). The UV-visible spectra of films were recorded using a Shimadzu UV-2101 PC spectrometer equipped with an integrating sphere.

**Table 2**  
Formulations under study.

Sample	NS content (wt.%)	HOBP content (wt.%)	TPP content (wt.%)
PP01NS	0.100	–	–
PP01HOBP	–	0.100	–
PP01TPP	–	–	0.100
PP01NSHOBP*	0.050	0.050	–
PP01NSHOBP	0.050	0.050	–
PP02NSHOBP	0.100	0.100	–
PP01NSTPP	0.050	–	0.050
PP02NSTPP	0.100	–	0.100

\* Sample prepared by mixing together PP, NS and HOBP, without previously mixing nanospheres and stabilizer.

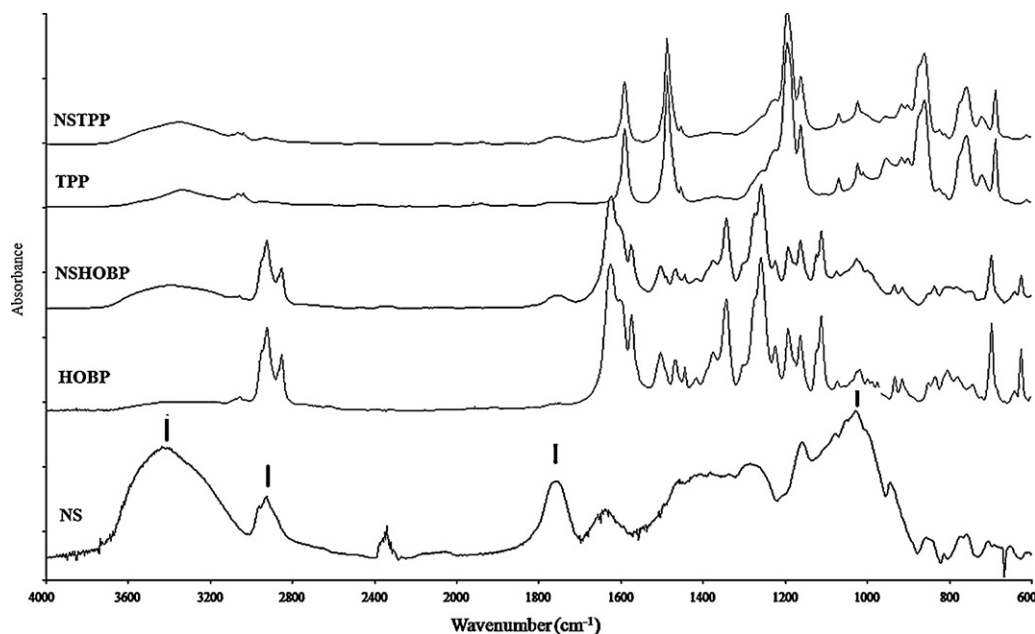


Fig. 2. FTIR spectra of nanosponges, stabilizers and their mixtures.

### 3. Results and discussion

#### 3.1. Spectroscopic characterization of NS, stabilizers and their pairs

FTIR spectra of the NS sample, the two stabilizers and their binary combinations, respectively, are plotted in Fig. 2. Nanosponges show a not well resolved spectrum, characterized by low intensity; nevertheless, it is very similar to that of single  $\beta$ -cyclodextrins (Belyakov et al., 2005). Indeed, with the exception of the typical band at  $1760\text{ cm}^{-1}$ , due to carbonyl group of carbonate bridges linking cyclodextrin units, it is possible to observe the symmetrical and asymmetrical vibration modes of methylene groups at  $2920\text{ cm}^{-1}$ , close to the stretching of hydroxyl group at  $3300\text{ cm}^{-1}$ , the stretching of ether group at  $1160\text{ cm}^{-1}$  and of carbon skeleton at  $1029\text{ cm}^{-1}$  (Belyakov et al., 2005). Referring to HOBP, its FTIR spectrum reports the characteristic signals of a hydroxyl benzophenone, in which it is possible to assign absorbance bands correspond-

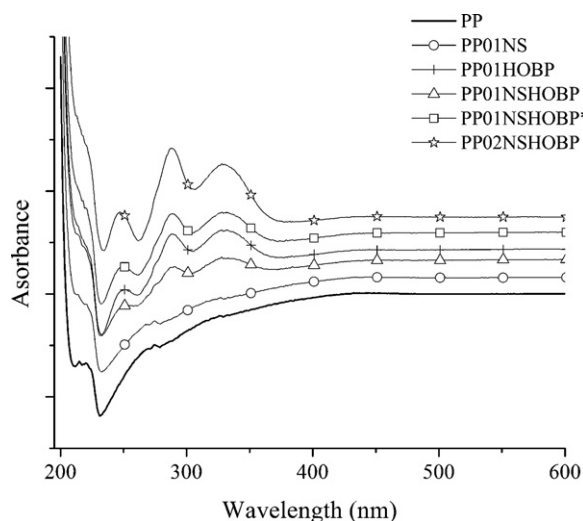


Fig. 3. UV-visible spectra of unloaded and loaded PP films.

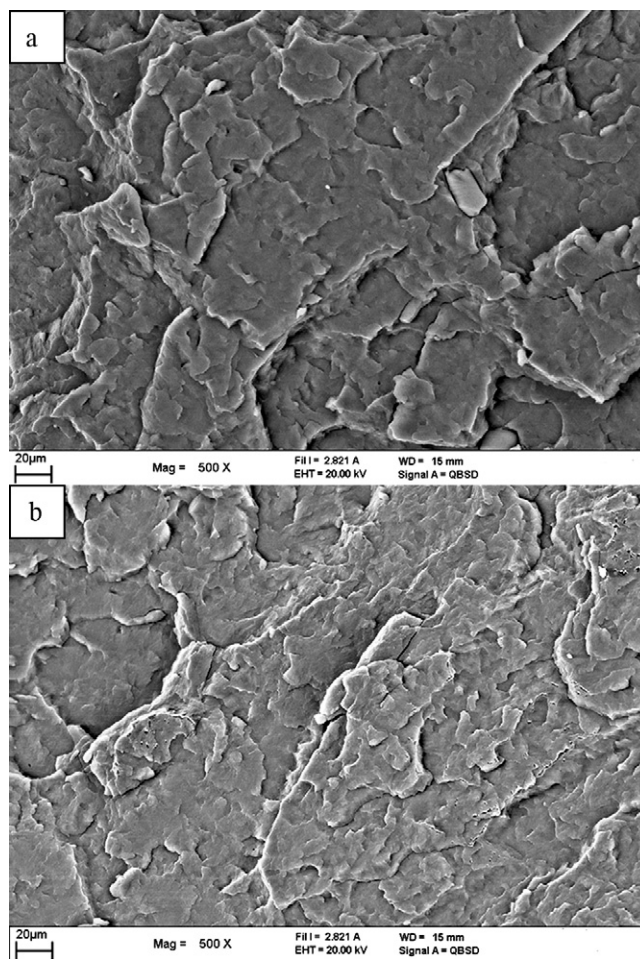


Fig. 4. SEM magnifications of PP01NS (a) and PP01NSTPP (b).



ing to O–H stretching at  $3300\text{ cm}^{-1}$ , aromatic C–H stretching at  $3060\text{ cm}^{-1}$ , aliphatic  $\text{CH}_3$  stretching at  $2900\text{ cm}^{-1}$ , C–H stretching of the alkoxy group O– $\text{CH}_2$ –R at  $2850\text{ cm}^{-1}$ , C=O stretching at  $1620\text{ cm}^{-1}$ , O–C=C stretching at  $1570\text{ cm}^{-1}$ , plus three bands from  $1450$  to  $1550\text{ cm}^{-1}$  attributed to C=C stretching of the aromatic group, and Ph–O–R stretching of ether group at  $1345$  and  $1260\text{ cm}^{-1}$ . The FTIR spectrum of HOBP-based pair is a perfect overlapping of the spectra of the components, and, indeed, it is possible to distinguish all bands of both constituents.

As far as TPP is considered, as already demonstrated in a previous work (Alongi et al., 2010), signals relative to aryl  $\text{CH}_2$  stretching

( $3060\text{ cm}^{-1}$ ), aryl C=C stretching ( $1600\text{ cm}^{-1}$ ), P–O–Ar stretching ( $1230$  and  $1160\text{ cm}^{-1}$ ), P–O–C skeleton stretching ( $1000$  and  $750\text{ cm}^{-1}$ ) and P–O–C stretching ( $790\text{ cm}^{-1}$ ) can be distinguished. Considering the spectrum of NS/TPP pair, it is possible to reach the same conclusions as for the pair containing HOBP: a perfect overlapping of signals coming from each component is observable.

The UV spectra of polypropylene and nanosponge-containing polypropylene clearly show the presence of a hindered amine-based antioxidant, already present in the neat polyolefin, with a typical absorbance at ca. 211 and 232 nm (Fig. 3). This stabilizer could affect the photooxidation of the formulations under

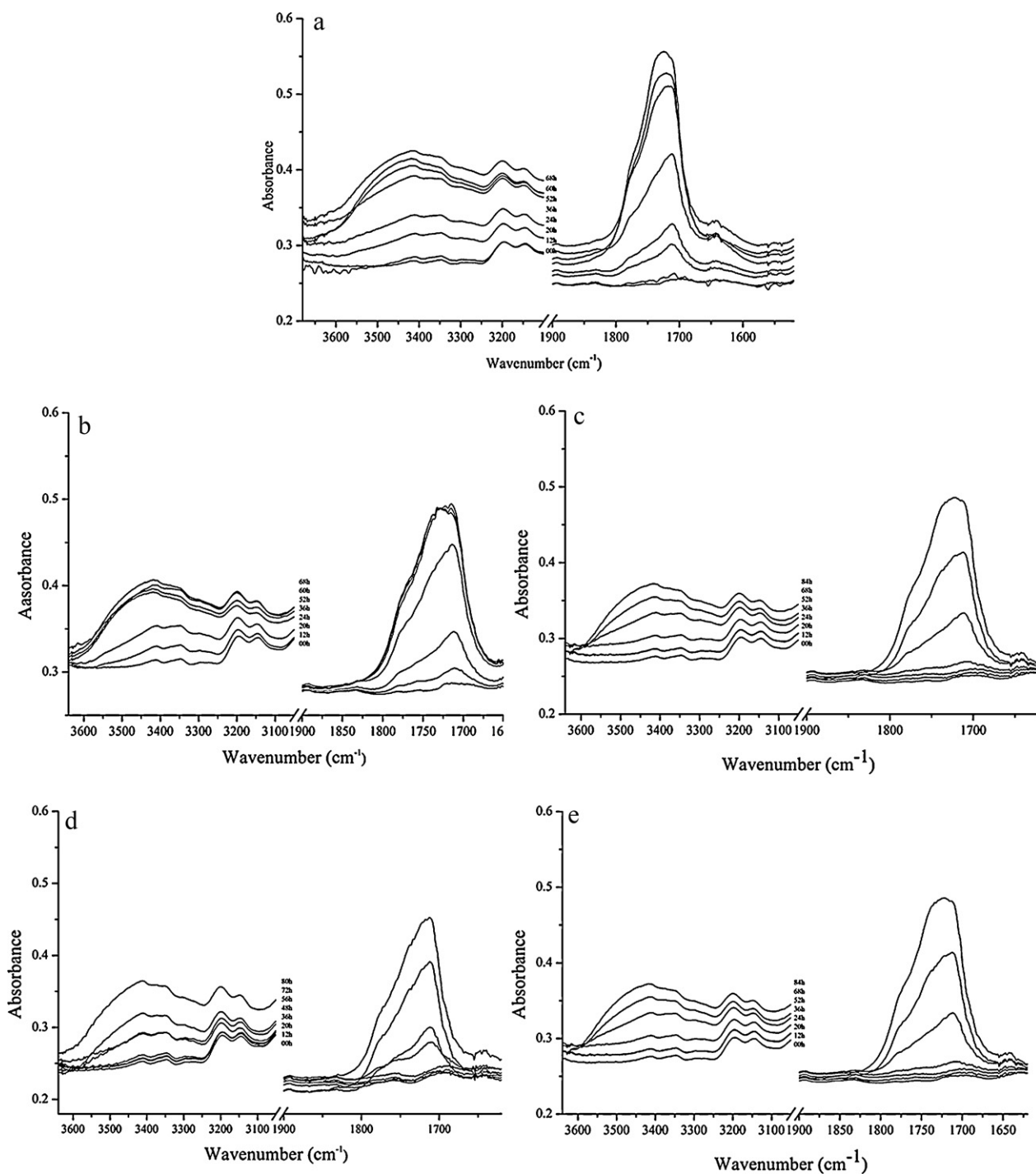


**Fig. 5.** FTIR spectra of a neat PP film (a) and of PP films containing 0.1 wt.% of NS (b), HOBP (c), TPP (d) and NSHOBP (e) photooxidized at  $\lambda > 300\text{ nm}$  in the regions of  $3600$ – $3000$  and  $1900$ – $1600\text{ cm}^{-1}$ .

study due to possible in the reactions with NS, as evidenced by its absorbance shifting to higher wavelengths.

On the other hand, HOBP-based PP film presents the typical absorbances of an aromatic compound at 232, 262 and 303 nm.

As far as the morphology of NS-based samples is considered, the electron microscopy has detected a fine and homogeneous dispersion of the nanoparticles within the polymer matrix, as shown by two SEM magnifications of PP01NS and PP02NSHOBP, respectively (Fig. 4).

### 3.2. Photooxidation of PP films

As well reported in the literature, the photooxidative degradation mechanism of a polymer (in this framework isotactic PP) can be easily studied by IR and UV–visible spectroscopies monitoring its structural changes and evaluating the formation of photodegradation products.

The evolution of unloaded PP structure in terms of infrared characterization during the irradiation exposure is reported in Fig. 5a. According to the literature (Bocchini et al., 2007, 2008; Diagne et al., 2005, 2006, 2007; Ding & Qu, 2006; Lonkar et al., 2010; Morlat et al., 2004; Morlat-Therias et al., 2005a; Qin et al., 2005), the shape of FTIR bands in spectra recorded after exposure of the various samples to UV light in ambient atmosphere have revealed remarkable changes of the material chemical structure. As shown in Fig. 5a, an increase of absorbance has been observed in two spectral domains of PP corresponding to the hydroxyl (at  $3400\text{ cm}^{-1}$ ) and carbonyl (at  $1717\text{ cm}^{-1}$ ) stretching vibration modes. This trend is in agreement with what has been found in the literature, i.e. the photooxidation of polypropylene results in the formation of hydroxyl (mainly hydroperoxides and alcohols) and carbonyl groups, easily detectable in the  $3200\text{--}3600$  and  $1600\text{--}1800\text{ cm}^{-1}$  region, respectively (Morlat-Therias et al., 2005a). More in detail, in the region centered at around  $1717\text{ cm}^{-1}$ , it is possible to distinguish some signals of photoproducts identified as  $\alpha$ -methylated carboxylic acids, esters, and  $\gamma$ -lactones at  $1715$ ,  $1735$  and  $1770\text{ cm}^{-1}$ , respectively. As a matter of fact, the attribution of the band at  $1735\text{ cm}^{-1}$  is still open to debate: indeed, it is postulated to result either from the carbonyl group of esters (Geuskens & Kabamba, 1987) or from the carbonyl vibration of carboxylic acids associated with hydroxyl groups (Swern, Witnauer, Eddy, & Parker, 1955).

### 3.3. Photooxidation of NS and NS/stabilizer-based PP composites

The FTIR spectra recorded during photooxidation of the NS-based PP nanocomposite film have shown notable changes. The main modifications of these spectra upon irradiation in the presence of oxygen are an increase of absorbance in the two domains of infrared region corresponding to the hydroxyl and carbonyl regions (Fig. 5b). The shape of the oxidation bands are similar to that observed for polypropylene film (Fig. 5a). Furthermore, when comparing Fig. 5a with b, the relative intensities of both bands are similar to those reported in the case of neat PP. Analogous considerations can be argued for films containing HOBP (Fig. 5c) and TPP (Fig. 5d) as well as when NS are mixed with stabilizers. Referring to the overall content of nanosponges and stabilizers, two different ratios (0.1 and 0.2 wt.%, respectively) have been investigated (namely, PP01NSHOBP and PP02NSHOBP, PP01NSTPP and PP02NSTPP) and negligible variations have been observed. As an example, FTIR spectrum of photooxidized PP02NSHOBP film is plotted in Fig. 5e.

This finding points out that the mechanism of polymer oxidation is not modified by the presence of nanosponges.

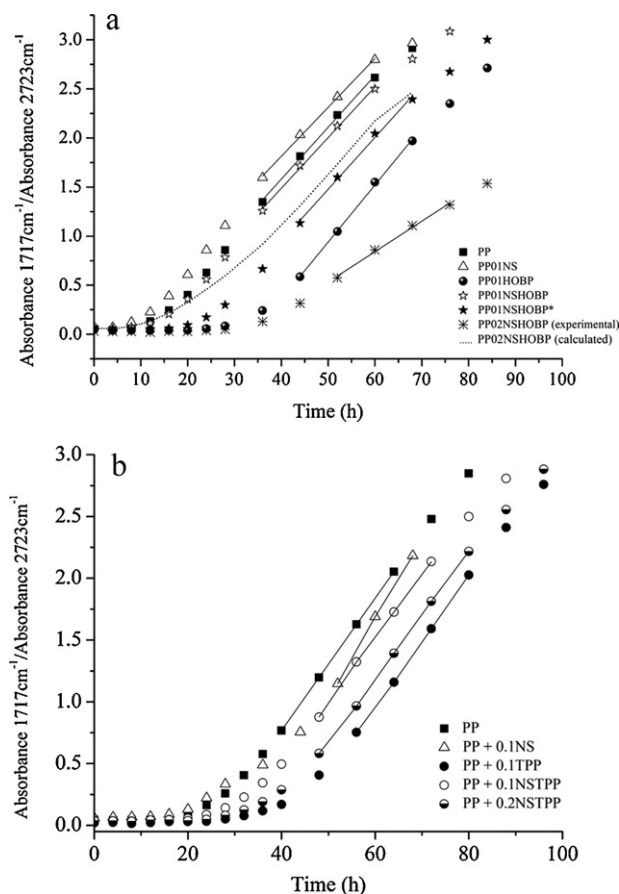


Fig. 6. Change of absorbance as a function of irradiation time for films photooxidized at  $\lambda > 300\text{ nm}$  of unloaded PP, NS- and HOBP-loaded PP (a), and NS- and TPP-loaded PP (b).

### 3.4. Rate of photooxidation of NS and NS/stabilizer-based PP composites

The kinetic curves of oxidation detected by infrared spectroscopy have been plotted in Fig. 6(a and b). Because of a slightly different thickness of the various films, the absorbance of each signal has been normalized to the band at  $2723\text{ cm}^{-1}$ , as mentioned in Section 2.

The increase of absorbance vs. irradiation time has been measured at the maximum of the carbonyl band centered at  $1717\text{ cm}^{-1}$  for PP films containing either NS, or stabilizers, or their mixtures. All the plotted curves are characterized by a more or less extended induction period, during which no oxidation of the polymer is observed thanks to an unknown processing stabilizer present in it. This aspect has already been observed in the UV–visible characterization of neat PP (Fig. 3). When NS, or stabilizers, or their mixtures are added to the polymer matrix, the above induction time turns out to be strongly dependent on the type of sample, as shown in Table 3 where the Oxidation Induction Time (OIT) and the subsequent rate of photooxidation are collected for all the formulations under study.

Generally, it is possible to observe that NS and stabilizers together affect drastically the OIT, while the photooxidation rate of PP (calculated as the slope of the interpolating curve in Fig. 6) remains almost constant within the experimental error, with the exception of PP02NSHOBP.

When nanosponges alone are added to polypropylene, they turn out to be ineffective to prevent its photodegradation: indeed, the OIT of PP is decreased from 12 down to 8 h, whereas HOBP and

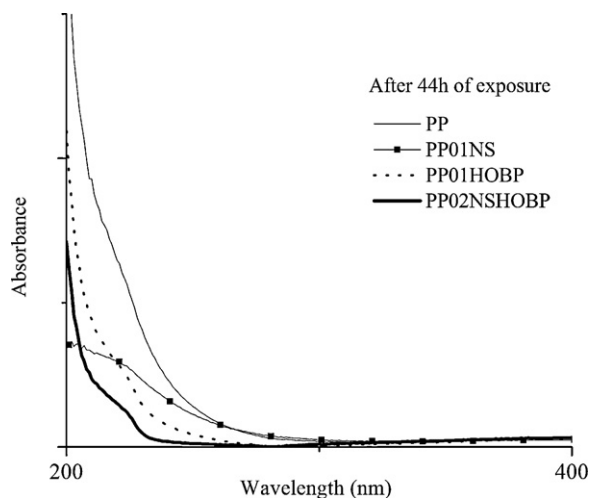


Fig. 7. UV-visible spectra of unloaded and loaded PP films photooxidized for 44 h at  $\lambda > 300$  nm.

**Table 3**

Oxidation induction time (OIT) and photooxidation rate of NS and NS/stabilizer-based PP films.

Sample	OIT (h)	Rate ( $\text{h}^{-1} \times 10^{-2}$ )
PP	12	$5.2 \pm 0.2$
PP01NS	8	$5.4 \pm 0.2$
PP01HOBP	28	$5.8 \pm 0.2$
PP01NSHOBP*	16	$6.1 \pm 0.1$
PP01NSHOBP	16	$5.4 \pm 0.1$
PP02NSHOBP	38	$1.1 \pm 0.1$
PP01TPP	32	$5.2 \pm 0.1$
PP01NSTPP	24	$5.1 \pm 0.1$
PP02NSTPP	28	$5.2 \pm 0.1$

\* Sample prepared by mixing together PP, NS and HOBP, without previously mixing nanosponges and stabilizer.

TPP are able to increase it from 12 up to 28 h and 32 h, respectively (Table 3).

On the other hand, by mixing NS with HOBP, OIT results to be dependent on the overall content of the mixture: indeed, if the concentration is low, namely 0.1 wt.% (PP01NSHOBP and PP01NSHOBP\*), OIT of PP is slightly increased (16 vs. 12 h). On the contrary, when the employed concentration is doubled (PP02NSHOBP), a significant increase of OIT (38 vs. 12 h) and a

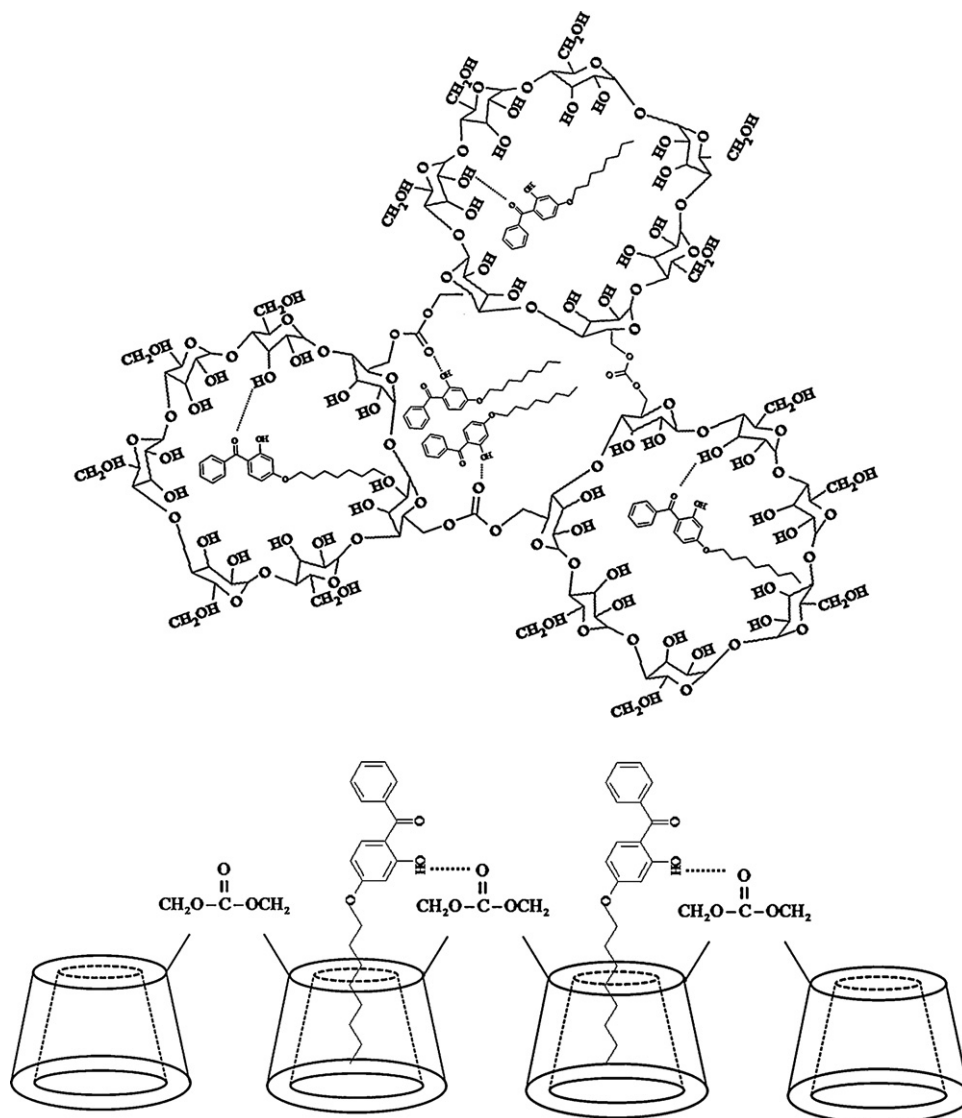


Fig. 8. Schematic representation of the interactions between NS and HOBP molecules.

remarkable decrease of photooxidation rate ( $1.1$  vs.  $5.2 \times 10^{-2} \text{ h}^{-1}$ ) have been recorded.

The same OIT value for PP01NSHOBP and PP01NSHOBP\* show that the preparation method of the NS/stabilizer pair does not affect the induction time.

In the same graph (Fig. 6a), the calculated curve of PP02NSHOBP has been added and compared with the experimental curve. The calculated curve has been plotted evaluating the contribution of each species independently, on the basis of additivity rules. The comparison between these two curves shows that a possible synergistic effect between the two species may exist, as the experimental curve does not overlap with the calculated one. If the above two species do not interact at all, the OIT should be shorter than recorded (theoretically 8 or 28 h, in relation to the highest contribution of NS or HOBP, respectively). On the contrary, the experimental OIT of this sample is higher (38 h) and this evidences and supports a synergistic action between NS and HOBP.

This hypothesis has been confirmed by comparing the UV–visible spectra of PP01NS, PP01HOBP and PP02NSHOBP after 44 h of exposure: as shown in Fig. 7, after this period, the HOBP is still present within the polymer matrix and is able to slow down the photooxidation kinetics of polypropylene (indeed, OIT of PP02NSHOBP is increased as referred to that of PP and PP01HOBP). This can be explained by hypothesizing that a fraction of the loaded HOBP has been entrapped within the cavities of nanosponges and, in this manner, protected by this network.

Although it is very difficult to establish a proper hypothesis to explain the interaction mechanism, the most plausible reason seems to be attributable to the formation of hydrogen bonds between the carbonyl group of HOBP and the hydroxyl groups of cyclodextrin and between the hydroxyl group of HOBP and the carbonyl group of the carbonate bridges. It is possible to suppose that HOBP has been directly entrapped within the truncated cone cavities of cyclodextrins or stays within the cavities of nanosponges that form the network. A scheme that could describe these interactions has given in Fig. 8.

Diametrically opposite is the trend when NS are combined with TPP (Fig. 6b). Indeed, when TPP acts alone, the OIT of polypropylene increases from 12 up to 32 h; on the contrary, in combination with NS, the OIT decreases from 32 down to 24 h and 28 h, in relation to the overall content. The above results underline that the use of this pair is not advantageous if compared with TPP alone.

#### 4. Conclusions

In the present paper, the photooxidation of polypropylene-based composites containing  $\beta$ -cyclodextrin nanosponges has been studied by monitoring the structural changes of the polymer matrix and evaluating the formation of photodegradation products through IR and UV–visible spectroscopies. Furthermore, the influence and the role of two stabilizers (namely, 2-hydroxy-4(octyloxy)-benzophenone and triphenyl phosphite) combined with nanosponges on the photooxidation of polypropylene-based composites exposed to UV light has been investigated.

The main results collected have been: (i) a significant reduction of the oxidation induction time in presence of  $\beta$ -cyclodextrin nanosponges alone; (ii) a remarkable OIT increase when nanosponges are combined with 2-hydroxy-4(octyloxy)-benzophenone; (iii) a possible synergistic effect between the two species, probably due to some chemical interactions; (iv) a low OIT when triphenyl phosphite is employed in combination with nanosponges. This pair turned out to be less efficient than TPP alone.

#### Acknowledgements

The authors would like to thank Prof. Giovanni Camino and Dr. Sergio Bocchini for the fruitful discussions.

#### References

- Alongi, J., Poskovic, M., Frache, A., & Trotta, F. (2010). Novel flame retardants containing cyclodextrin nanosponges and phosphorus compounds to enhance EVA combustion properties. *Polymer Degradation and Stability*, 95, 2093–2100.
- Belyakov, V. N., Belyakova, L. A., Varvarin, A. M., Khora, O. V., Vasilyuk, S. L., Kazdobin, K. A., Maltseva, T. V., Kotvitsky, A. G., & Danil de Namor, A. F. (2005). Super-molecular structures on silica surface and their adsorptive properties. *Journal of Colloid and Interface Science*, 285, 18–26.
- Bocchini, S., Morlat-Therias, S., Gardette, J.-L., & Camino, G. (2007). Influence of nanodispersed boehmite on polypropylene photooxidation. *Polymer Degradation and Stability*, 92, 1847–1856.
- Bocchini, S., Morlat-Therias, S., Gardette, J.-L., & Camino, G. (2008). Influence of nanodispersed hydrotalcite on polypropylene photooxidation. *European Polymer Journal*, 44, 3473–3481.
- Bocchini, S., Fukushima, K., Di Blasio, A., Fina, A., Frache, A., & Geobaldo, F. (2010). Poly-lactic acid and polylactic acid-based nanocomposites photooxidation. *Biomacromolecules*, 11, 2919–2926.
- Boscolo, B., Trotta, F., & Ghibaudi, E. (2010). High catalytic performances of Pseudomonas fluorescens lipase adsorbed on a new type of cyclodextrin-based nanosponges. *Journal of Molecular Catalysis B-Enzymatic*, 62, 155–161.
- Botta, L., Dintcheva, N. T., & La Mantia, F. P. (2009). The role of organoclay and matrix type on photo-oxidation of polyolefin/clay nanocomposite films. *Polymer Degradation and Stability*, 94, 712–718.
- Bottino, F. A., Di Pasquale, G., Fabbri, E., Orestano, A., & Pollicino, A. (2009). Influence of montmorillonite nano-dispersion on polystyrene photo-oxidation. *Polymer Degradation and Stability*, 94, 369–374.
- Cavalli, R., Trotta, F., & Tumiatti, W. (2006). Cyclodextrin-based nanosponges for drug delivery. *Journal of Inclusion Phenomena Macrocyclic Chemistry*, 56, 209–213.
- Chen, X. D., Wang, Z., Liao, Z. F., Mai, Y. L., & Zhang, M. Q. (2007). Roles of anatase and rutile TiO<sub>2</sub> nanoparticles in photooxidation of polyurethane. *Polymer Testing*, 26, 202–208.
- Di Nardo, G., Roggero, C., Campolongo, S., Valetti, F., Trotta, F., & Gilardi, G. (2009). Catalytic properties of catechol1, 2-dioxygenase from *Acinetobacter radiore-sistens* S13 immobilized on nanosponges. *Dalton Transactions*, 33, 6507–6512.
- Diagne, M., Gueye, M., Vidal, L., & Tidjani, A. (2005). Thermal stability and fire retardant performance of photo-oxidized nanocomposites of polypropylene-graft-maleic anhydride/clay. *Polymer Degradation and Stability*, 89, 418–426.
- Diagne, M., Gueye, M., Dasilva, A., Vidal, L., & Tidjani, A. (2006). The effect of photo-oxidation on thermal and fire retardancy of polypropylene nanocomposites. *Journal of Materials Science*, 41, 7005–7010.
- Diagne, M., Gueye, M., Dasilva, A., & Tidjani, A. (2007). Comparative photo-oxidation under natural and accelerated conditions of polypropylene nanocomposites produced by extrusion and injection molding. *Journal of Applied Polymer Science*, 105, 3787–3793.
- Ding, P., & Qu, B. (2006). Synthesis of exfoliated PP/LDH nanocomposites via melt-intercalation: structure, thermal properties and photo-oxidative behavior in comparison with PP/MMT nanocomposites. *Polymer Engineering and Science*, 46, 1153–1159.
- Geuskens, G., & Kabamba, M. S. (1987). Photo-oxidation of polymers: Part X—The photo-oxidation of an ethylene–propylene copolymer initiated by benzophenone. *Polymer Degradation and Stability*, 19, 315–322.
- Kojima, Y., Usuki, A., Kawasumi, M., Okada, A., Fukushima, Y., Karauchi, T., & Kamigaito, O. (1993). Synthesis of nylon 6-clay hybrid. *Journal of Materials Research*, 8, 1179–1184.
- Kumanayaka, T. O., Parthasarathy, R., & Jollands, M. (2010). Accelerating effect of montmorillonite on oxidative degradation of polyethylene nanocomposites. *Polymer Degradation and Stability*, 95, 672–676.
- Leroux, F., Meddar, L., Mailhot, B., Morlas-Therias, S., & Gardette, J.-L. (2005). Characterization and photooxidative behaviour of nanocomposites formed with polystyrene and LDHs organo-modified by monomer surfactant. *Polymer*, 46, 3571–3578.
- Lonkar, S. P., Therias, S., Caperaa, N., Leroux, F., & Gardette, J.-L. (2010). Photooxidation of polypropylene/layered double hydroxide nanocomposites: Influence of intralamellar cations. *European Polymer Journal*, 46, 1456–1464.
- Magagula, B., Nhalpo, N., & Focke, W. M. (2009). Mn<sub>2</sub>Al-LDH and Co<sub>2</sub>Al-LDH-stearate as photodegradants for LDPE film. *Polymer Degradation and Stability*, 94, 947–954.
- Mailhot, B., Morlat-Therias, S., Bussiere, P. O., Le Pluart, L., Duchet, J., Sautereau, H., Gerard, J.-F., & Gardette, J.-L. (2008). Photoageing behaviour of epoxy nanocomposites: comparison between spherical and lamellar nanofillers. *Polymer Degradation and Stability*, 93, 1786–1792.
- Morlat, S., Mailhot, B., Gonzalez, D., & Gardette, J.-L. (2004). Photo-oxidation of polypropylene/montmorillonite nanocomposites. 1. Influence of nanoclay and compatibilizing agent. *Chemistry of Materials*, 16, 377–383.
- Morlat-Therias, S., Mailhot, B., Gonzalez, D., & Gardette, J.-L. (2005). Photo-oxidation of polypropylene/montmorillonite nanocomposites. 2. Interactions with stabilizers. *Chemistry of Materials*, 17, 1072–1078.



- Morlat-Therias, S., Mailhot, B., Gardette, J.-L., Da Silva, C., Haidar, B., & Vidal, A. (2005). Photooxidation of ethylene-propylene-diene/montmorillonite nanocomposites. *Polymer Degradation and Stability*, 90, 78–85.
- Morlat-Therias, S., Fanton, E., Gardette, J.-L., Dintcheva, N. T., La Mantia, F. P., & Malatesta, V. (2008). Photochemical stabilization of linear low-density polyethylene/clay nanocomposites: towards durable nanocomposites. *Polymer Degradation and Stability*, 93, 1776–1780.
- Okada, A., & Usuki, A. (2006). Twenty years of polymer-clay nanocomposites. *Macromolecular Materials Engineering*, 291, 1449–1476.
- Philippart, J. L., Sinturel, C., & Gardette, J.-L. (1995). Influence of light intensity on the photooxidation of polypropylene. *Polymer Degradation and Stability*, 58, 261–268.
- Pinnavaia, T. J., & Beall, G. (2001). *Polymer-clay nanocomposites* (1st ed.). New York: John Wiley & Sons.
- Qin, H., Zhao, C., Zhang, S., Chen, G., & Yang, M. (2003). Photo-oxidative degradation of polyethylene/montmorillonite nanocomposites. *Polymer Degradation and Stability*, 81, 497–500.
- Qin, H., Zhang, Z., Feng, M., Gong, F., Zhang, S., & Yang, M. (2004). The influence of interlayer cations on the photo-oxidative degradation of polyethylene/montmorillonite composites. *Journal of Polymer Science Part B: Polymer Physics*, 42, 3006–3012.
- Qin, H., Zhang, S., Liu, H., Xie, S., Yang, M., & Shen, D. (2005). Photo-oxidative degradation of polypropylene/montmorillonite nanocomposites. *Polymer*, 46, 3149–3156.
- Ray, S. S., & Okamoto, M. (2003). Polymer/layered silicate nanocomposites: A review from preparation to processing. *Progress in Polymer Science*, 28, 1539–1641, and references quoted in.
- Swaminathan, S., Vavia, P. R., Trotta, F., & Torne, S. (2007). Formulation of betacyclodextrin based nanosponges of itraconazole. *Journal of Inclusion Phenomena Macrocyclic Chemistry*, 57, 89–94.
- Swaminathan, S., Cavalli, R., Trotta, F., Ferruti, P., Ranucci, E., Gerges, I., Manfredi, A., Marinotto, D., & Vavia, P. R. (2010). In vitro release modulation and conformational stabilization of a model protein using swellable polyamidoamine nanosponges of beta-cyclodextrin. *Journal of Inclusion Phenomena and Macrocyclic Chemistry*, 68, 183–191.
- Swaminathan, S., Pastero, L., Serpe, L., Trotta, F., Vavia, P. R., Aquilano, D., Trotta, M., Zara, G., & Cavalli, R. (2010). Cyclodextrin-based nanosponges encapsulating camptothecin: Physicochemical characterization, stability and cytotoxicity. *European Journal of Pharmaceutics and Biopharmaceutics*, 74, 193–201.
- Swern, D., Witnauer, I. P., Eddy, C. R., & Parker, W. E. (1955). Peroxides III. Structure of aliphatic peracids in solution and in the solid state. An infrared, X-ray diffraction and molecular weight study. *Journal of American Chemical Society*, 77, 5537–5541.
- Torne, S. J., Ansari, K. A., Vavia, P. R., Trotta, F., & Cavalli, R. (2010). Enhanced oral paclitaxel bioavailability after administration of paclitaxel-loaded nanosponges. *Drug Delivery*, 17, 419–425.